REPO

AD-A227 453

1a REPORT SECURITY CLASSIFICATION UNCLASSIFIED		
2a SECURITY CLASSIFICATION AUTHORITY		REPORT
2b DECLASSIFICATION/DOWNGRADING SCHEDULE		Approved for public release

4 PERFORMING ORGANIZATION REPORT NUMBER(S) Number 5		5 MONITORING ORGANIZATION REPORT NUMBER(S) N00014-89-J-1197

6a NAME OF PERFORMING ORGANIZATION High Temperature Gasdynamics Lab Stanford Universtiy	6b OFFICE SYMBOL (If applicable)	7a NAME OF MONITORING ORGANIZATION Office of Naval Research Dr. Robert Schwartz
6c ADDRESS (City, State, and ZIP Code) Mechanical Engineering Dept. Stanford, CA 94305-3032		7b ADDRESS (City, State, and ZIP Code) Code 373 Naval Weapons Center China Lake, CA 93555-6001

8a NAME OF FUNDING/SPONSORING ORGANIZATION Office of Naval Research	8b OFFICE SYMBOL (If applicable)	9 PROCUREMENT INSTRUMENT IDENTIFICATION NUMBER

| 8c ADDRESS (City, State, and ZIP Code) 800 North Quincy Street Arlington, VA 22217-5000 | | 10 SOURCE OF FUNDING NUMBERS |

PROGRAM ELEMENT NO.	PROJECT NO.	TASK NO	WORK UNIT NO

11 TITLE (Include Security Classification)
On the Development of In-Situ Raman Analysis of Plasma Deposited Diamond

12 PERSONAL AUTHOR(S) M.A. Cappelli and H. Herchen

13a TYPE OF REPORT Technical	13b TIME COVERED FROM _____ TO _____	14 DATE OF REPORT (Year, Month, Day) 1990	15 PAGE COUNT 7

16 SUPPLEMENTARY NOTATION

17 COSATI CODES			18 SUBJECT TERMS (Continue on reverse if necessary and identify by block number)
FIELD	GROUP	SUB-GROUP	

19 ABSTRACT (Continue on reverse if necessary and identify by block number)

Progress towards the development of in-situ Raman capabilities for plasma deposited diamond films is described. The shift and broadening of the first order Raman-active phonon mode in natural and synthetic diamond is analyzed at temperatures within the range commonly employed in vapor phase diamond deposition (>1000K). At these temperatures, we have found that the anti-Stokes component to the Raman signature can be detected and employed as an alternative diagnostic. We describe preliminary results in which in-situ Raman is employed to monitor the temperature of a heated natural diamond substrate exposed to both molecular and atomic hydrogen. We find that variations in molecular hydrogen fraction in the reactant gas mixture can lead to substantial variation in substrate temperature. Following exposure to atomic hydrogen, the Raman line center is found to be shifted to lower energy (at ambient temperatures). The shift is in part attributed to the presence of interstitial hydrogen.

20 DISTRIBUTION/AVAILABILITY OF ABSTRACT ☒ UNCLASSIFIED/UNLIMITED ☐ SAME AS RPT ☐ DTIC USERS	21 ABSTRACT SECURITY CLASSIFICATION Unclassified
22a NAME OF RESPONSIBLE INDIVIDUAL	22b TELEPHONE (Include Area Code) 22c OFFICE SYMBOL

DD FORM 1473, 84 MAR 83 APR edition may be used until exhausted
All other editions are obsolete

ON THE DEVELOPMENT OF IN-SITU RAMAN ANALYSIS
FOR PLASMA DEPOSITED DIAMOND

MARK A. CAPPELLI AND H. HERCHEN

High Temperature Gasdynamics Laboratory
Stanford University, Stanford. California 94305

ABSTRACT

Progress towards the development of in-situ Raman capabilities for plasma deposited diamond films is described. The shift and broadening of the first order Raman-active phonon mode in natural and synthetic diamond is analyzed at temperatures within the range commonly employed in vapor phase diamond deposition (>1000K). At these temperatures, we have found that the anti-Stokes component to the Raman signature can be detected and employed as an alternative diagnostic. We describe preliminary results in which in-situ Raman is employed to monitor the temperature of a heated natural diamond substrate exposed to both molecular and atomic hydrogen. We find that variations in molecular hydrogen fraction in the reactant gas mixture can lead to substantial variation in substrate temperature. Following exposure to atomic hydrogen, the Raman line center is found to be shifted to lower energy (at ambient temperatures). The shift is in part attributed to the presence of interstitial hydrogen.

INTRODUCTION

Raman scattering has become a standard method of characterizing low pressure plasma deposited diamond film [1-4]. The scattering features in the vicinity of both the Raman active first-order phonon mode in diamond at approximately 1332 cm^{-1} [5-7] and graphite at approximately 1580 cm^{-1} [8] have provided the basis for interpreting the composite nature of synthetic diamond films [9]. Raman scattering is traditionally employed ex-situ, quite often with micro-positioning and focusing, and large solid angle detection [10]. Micro-Raman, as it is commonly called, is necessary in part to compensate for the relatively low scattering efficiencies (typically $10^{-6} - 10^{-7}$ [11]) of most crystals. Although micro-Raman is capable of probing spatial features with micron-size resolution, the more conventional macro-Raman analysis, with a relatively large laser spot size and a generally smaller collection solid angle gives a better indication of the "average" composition of the film.

In this paper, we discuss our progress at employing macro-Raman analysis as an in-situ diagnostic for plasma deposited diamond. This research is motivated by the need for reliable in-situ diagnostics for both deposited film and the gas phase, which will permit direct real-time correlation between deposit morphology and possible gas phase precursors. Real-time monitoring of both deposit structure and of species recognized as important precursors (i.e., CH_3 [12], C_2H_2 [13] and H [14-16]) together with detailed modelling of the complete deposition process are key elements of "intelligent processing" systems, soon to be designed for the efficient and optimum synthesis of diamond films.

A number of interrelated problems are encountered when attempting to employ Raman scattering in-situ. First, the Raman scattering behavior of diamond at elevated temperatures (>500K) is poorly understood. Quantum mechanical theories [17,18] predict the shift and broadening of the first-order Raman spectrum to increase with increasing temperature. These theories are at best qualitatively consistent with the general observations made in natural diamond by Nayar [19] and Krishnan [20] in the temperature range between 85K and 976K. Until now, there was no available data on the broadening above 976K, which is in the vicinity of the lower limit where plasma and hot-filament deposition of diamond is routinely performed. Indeed, these previous measurements [19,20] were plagued by poor signal to noise and signal to background interference at higher temperatures, the latter due to thermal radiation from the diamond itself.

140

The overall scattering efficiency at higher temperatures decreases in part as a result of the fact that one begins to populate higher vibrational energy states. This implies that at temperatures $T \simeq h\nu_s/k$ (here h and k are Planck's and Boltzmann's constant respectively. and ν_s represents the Raman shift), the scattering intensity of the anti-Stokes component is comparable to that of the Stokes component, suggesting that the Stokes to anti-Stokes component intensity ratio can be used as a high temperature calibrant. In addition, accurate knowledge of the the variation in the Raman shift with temperature suggests that the line center position of the Stokes or anti-Stokes components can also be used as a temperature calibrant. Accurate control of the substrate temperature in diamond film synthesis is found to be necessary in order to achieve desired film morphology [14,15].

The second problem encountered in attempting to make Raman scattering a useful in-situ diagnostic is one of scan acquisition time. Growth rates of 10-100 μm/h are now common in diffuse arc discharges [21,22]. Using these growth strategies to deposit 200 μm thick diamond plates, suitable for example, as microelectronic heat sinks, imply spectral scans much less than hours in duration.

The scan duration necessary to obtain a satisfactory signal to noise ratio is directly coupled to the optical collection efficiency. For practical reactor geometries, it will be difficult to do better than $f^\# = 1$ collection optics. In the experiments described below, $f^\# = 3 - 5$. In some cases, as for example, in studying homoepitaxy or heteroepitaxy, it may be desirable to observe the polarization anisotropy, which is less pronounced with increasing collection solid angle. In recent experiments performed by Yoshikawa, et al [23], the polarization anisotropy of the Raman scattering from a thin film of diamond deposited on c:BN was used to infer heteroepitaxial nucleation and an estimate of the tensile stress in the diamond film.

We can express the differentially scattered power $dI/d\Omega$ from a diamond sample as

$$\frac{dI}{d\Omega} = \sigma_\Omega I_0 \qquad (1)$$

(dimensions W/sr/atom), where σ_Ω is the differential Raman scattering cross section (cm^2 sr) and I_0 is the incident laser intensity (W/cm^2). The total scattered power collected onto the photodetector at the exit plane of a monochromator can be expressed as

$$I_R = \frac{dI}{d\Omega} d\Omega \, dV \, N \, T \qquad (2)$$

where $d\Omega$ represents the collection solid angle, dV the volume imaged onto the entrance slit of the monochromator, N the atomic density of diamond and T the optical transmission of the monochromator. If we take $\sigma_\Omega \simeq 10^{-31}$ cm^2/sr (approximately 10^{-5} times the corresponding Rayleigh scattering cross section), $I_0 \simeq 100$ W/cm^2 (cw laser), a film thickness of 5 mm, an image area of approximately 5×10^{-4} cm^2, $T \simeq 0.1$, and $f^\# \simeq 3$, we arrive at $I_R = 10^{-17}$ W, or approximately 3000 photons per second. This puts us in photon counting mode. One can show that for a spectral bandwidth of one wavenumber, this signal is easily obscured by a blackbody radiator at 2500K (2×10^9 photons per second). Although direct interference from a nearby source such as a hot filament or a hot cathode is unlikely, some contribution through plasma interference and scattering is likely. To overcome these interferences, we have employed gated detection by intensity modulating a cw argon-ion laser, or in some cases by using a pulsed diode-pumped Nd:YLF laser operating at 2 kHz. The signals are detected within gate intervals short enough to reject the continuous plasma interferences. Scan durations for these two scattering strategies are typically 10 minutes when using the argon-ion laser and a few minutes when using the Nd:YLF laser. Most of the experiments described below are on natural diamond substrates. Scan durations are expected to be somewhat longer for synthetic diamond films.

EXPERIMENTAL FACILITIES

Two separate reactor chambers were employed for the results described in this paper. In the first chamber, natural diamond is positioned onto an electrically heated molybdenum foil. The samples are excited by either a cw argon-ion laser (chopped at approximately 2 kHz) or a pulsed diode-pumped Nd:YLF laser (Spectra Physics Model 7200) at approximately 45° from the substrate normal. The scattered light (unanalyzed for its polarization) is collected along a direction normal to the surface and imaged onto the entrance slit of a 1 m grating monochromator. Bandpass and blocking filters are employed at the exit slits of the monochromator to minimize stray light. A Hamamatsu model R2801 photomultiplier tube mounted in a Peltier-cooled housing is used as the detector and is operated in a photon counting mode. Signals are analyzed by a Stanford Research Systems Model SR400 photon counter.

The second reaction chamber was originally constructed to study diamond growth in diffuse arc discharges. Natural diamond is mounted onto a resistively heated silicon wafer. A diffuse arc is formed between a hot, hollow, molybdenum cathode and the silicon wafer (which acts as the anode). Typical current - voltage discharge operating conditions are 3 A and 150 V at pressures of approximately 10 torr. The operating gas mixture in this reactor for experiments described below is either all argon or mixtures of argon and hydrogen, each of which are mass flow controlled. The incident laser is directed onto the sample at an angle of approximately 45° from the surface normal. The scattered light (unanalyzed for its polarization) is collected at an angle of approximately 90° to the incident light path. The remaining part of the optical processing is essentially the same as that for the first chamber. At sufficiently high temperatures (>1150K), the diamond temperature is estimated from the temperature of the resistively heated support filaments as measured with a disappearing filament pyrometer. The temperatures are estimated to be accurate to ±50K.

RESULTS

High Temperature Raman Scattering Properties of Diamond

Figure 1 shows typical Stokes and anti-Stokes Raman signals from natural type IIA diamond (2 mm × 2 mm × 250 μm, (100) polished face) at temperatures of 1370K and 1450K respectively. The diamond is heated as described above, in a low pressure argon atmosphere. These spectra were taken using the 526.2 nm output of the frequency doubled Nd:YLF laser. No significant heating by the pulsed laser is observed when the diamond sample is unheated. When employing the pulsed laser, shifts are estimated to be accurate to within 3 cm^{-1}, a limitation imposed by the mechanical jitter in the grating turret mount. When employing the 457.9 nm output from the argon-ion laser as an excitation source, an argon-ion emission line at 488.0 nm appears near the location of the Raman peak in diamond. This emission line provides an accurate calibration for the position of the line center frequency. In this case, the lineshifts are estimated to be accurate to within 0.6 cm^{-1}.

A number of experiments aimed at measuring the temperature dependence of the Raman line broadening were performed at lower temperatures (400K-1000K) with a spectral resolution of 0.8 cm^{-1} (HWHM). The temperatures were estimated from the data of Krishnan [20]. The results are displayed in Figure 2a along with the broadening measurements of Krishnan. Reasonable agreement between our results and that of Krishnan [20], is observed. Both our results and the results of Krishnan as displayed in Figure 2a are corrected for instrument broadening.

At higher temperatures, reasonably accurate temperatures can be determined by optical pyrometry. The Raman shifts were measured over the range of 1150K to 1460K. These shifts are compared to those measured at lower temperatures by Nayar [19] and Krishnan [20] in Figure 2b. Two observations can be made from this figure. First, the discrepancy in the data of Nayar and Krishnan is significant above 500K, as was originally pointed out by Krishnan
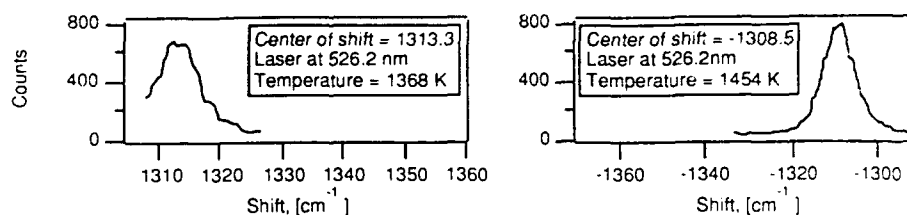
3

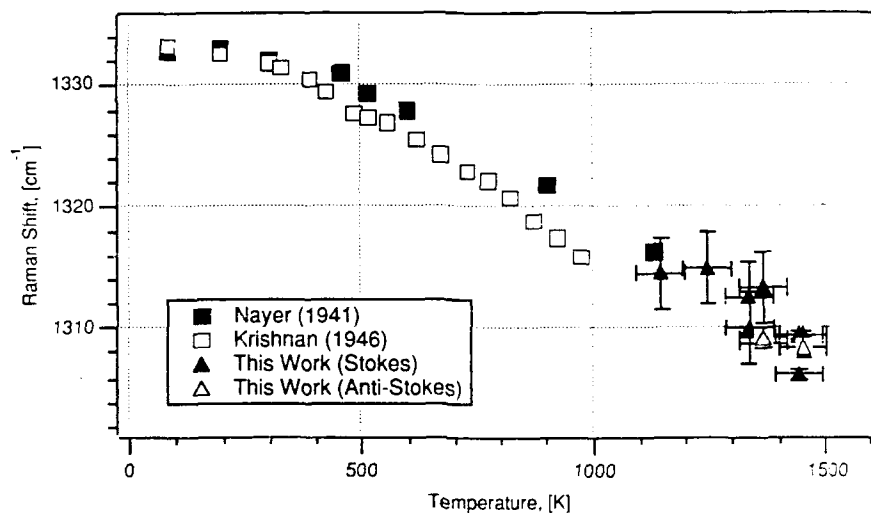Figure 1. Representative Stokes and Anti-Stokes Raman Spectra

Figure 2. Comparison of Data of Nayar, Krishnan, and This Work

[20]. Secondly, our data at temperatures above 1150 K best fit the extrapolated curve of Nayar [19], although no account of experimental uncertainties are given in that earlier work.

In – Situ Analysis of Heated Natural Diamond Exposed to Molecular Hydrogen

It is well known that plasma and filament enhanced diamond synthesis displays a sensitivity to the partial pressure of molecular hydrogen in the reactant gas mixture. This result is interpreted in terms of the important role atomic hydrogen, produced by plasma or filament activation, plays in the stabilization of diamond growth surfaces [15]. Variation in the reactant gas feed composition alone can change for example, the discharge characteristics and, as we will demonstrate here, the substrate temperature.

The heated natural diamond sample was exposed for approximately 45 minutes to unactivated argon. Within 8 minutes from the time of initial heating, the diamond sample stabilized to a temperature of 900K as estimated from the measured shift of the Stokes component in the Raman spectrum (Figure 3). The argon flow rate was set at 53 sccm and the pressure in the chamber was 9.2 torr. Raman spectra were taken at approximately 15 minute intervals. After the 45 minute exposure to argon, the argon was replaced by unactivated molecular hydrogen (194 sccm, 9.6 torr). The substrate temperature was found to fall and stabilize immediately at approximately 350K, as is evident from the sudden shift in the Raman peak to approximately 1330.5 cm^{-1}. This fall is attributed to the increased thermal conductivity of the gas stream. This is verified by the fact that no significant change was observed when the flow rates were reduced to 51 sccm, indicating that we are in a "creeping flow" regime as
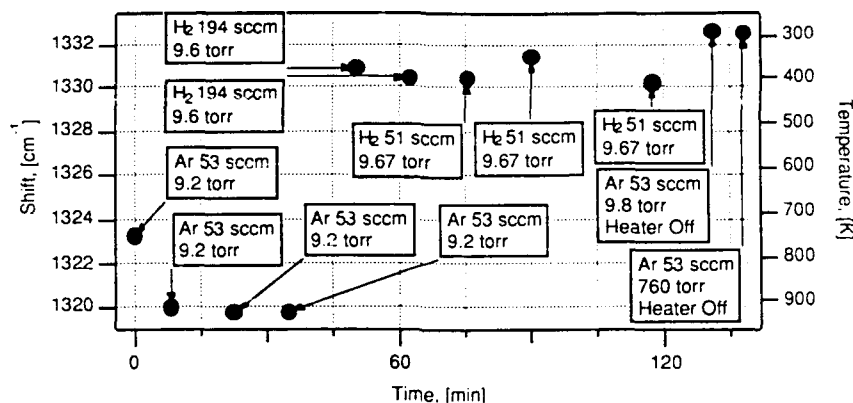
4

Figure 3. Heated Natural Diamond in Cold Argon or Hydrogen Flow

a result of the relatively low Reynolds number.

These observations have significant ramifications in process control of diamond film morphology. They imply that changes in the reactant gas mixture cannot be implemented without corrections to the substrate heating process. Any theoretical model used to describe the deposition process should in addition contain the appropriate energy equation with proper heat flux boundary conditions, if in practice, the surface temperature is not an independently controlled parameter.

In – Situ Analysis of Heated Natural Diamond Exposed to Plasma Activated Gases

In-situ Raman analysis was performed on natural diamond during exposure to plasma activated argon and hydrogen mixtures within the diffuse arc discharge. For the results described here, the diamond was heated by the plasma itself. The intensity modulated argon ion laser at 514.5 nm was used as an excitation source. Checks were performed so as to ensure that the argon-ion laser did not significantly contribute to the heating of the diamond sample.

In the absence of a discharge (argon only, 10 torr, 75 sccm), the Raman spectrum displays the characteristic unshifted peak centered at approximately 1332 cm^{-1} (Figure 4a). A Raman scan is taken approximately 1/2 hour following the initiation of a diffuse arc. This spectrum is displayed in Figure 4b. Notice that the overall scattering intensity, signal-to-noise, and signal to background ratios have decreased as a result of plasma heating and fluorescence interference. The temperature is estimated to be approximately 800K. The decrease in the scattering efficiency is attributed to a decrease in the average number of phonons occupy , the lowest vibrational state. The increase in the background interference is attributed to plasma fluorescence. This is graphically displayed in Figure 5, where the results of the Raman scan without intensity modulating the laser source is shown as the upper trace. As one can see, there is significant structure due to as yet unassigned plasma emission in the vicinity of the diamond peak. It is fortuitous that one of the sharper features does not directly overlap the diamond feature in this example. Gated detection (lower trace) conveniently extracts the signal that is attributed to Raman scattering from the diamond sample.

Figure 6a shows the Raman spectrum for conditions equal to that in Figure 4b, 1/2 hour later into the same experimental run. The two scans are essentially equal, suggesting that the conditions are stable and that the diamond sample is unaltered as a result of further argon plasma exposure. Finally, a Raman scan was taken following the addition of hydrogen (200 sccm H$_2$, 75 sccm Ar, 10 torr) into the gas stream (see Figure 6b). The discharge power was increased substantially in order to sustain the predominantly hydrogen discharge. This
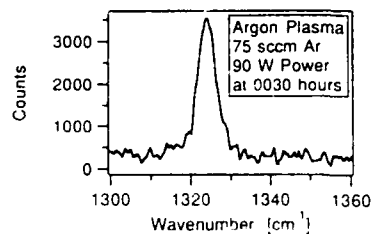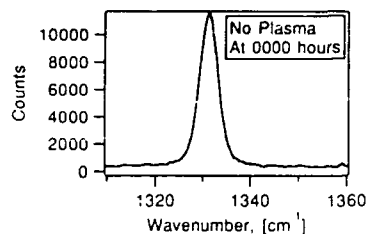
5

Figure 4a. Raman Line with No Plasma   Figure 4b. Raman Line with Plasma
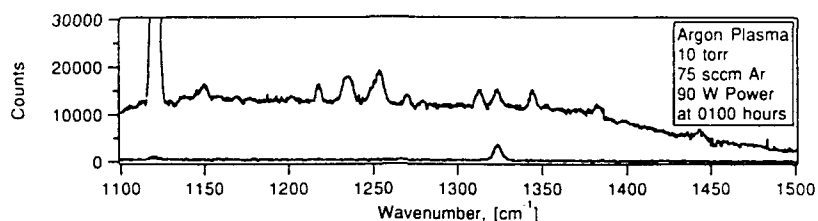

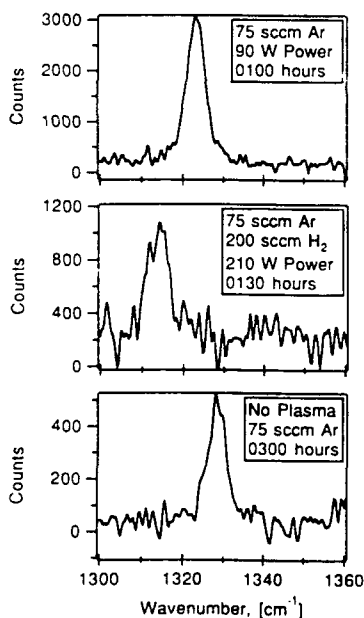Figure 5. Background Interference (Upper Trace) and Raman Signal (Lower Trace)

Figure 6a, 6b, 6c. In-Situ Raman
Signal under three Conditions

resulted in an increased heating of the diamond sample raising its temperature to approximately 1200K. The signal to noise drops in part as a result of a substantial increase in the plasma emission in the vicinity of the Stokes component. Following approximately one hour exposure to atomic hydrogen, a Raman scan was taken with the discharge off (Figure 6c). This scan is substantially different than the first scan (Figure 4a) prior to plasma exposure. Inspection of the diamond sample after its removal from the chamber indicated a slight discoloration, which could account for the reduced scattering intensity. The slight residual shift in the Raman peak to lower energy suggests that there is a residual strain in the diamond sample which may in part be due to interstitial hydrogen. We are in the process of repeating these experiments so as to develop a better understanding of these observations.

CONCLUDING REMARKS

The development of in-situ Raman analysis for plasma and filament deposited diamond films is discussed. Preliminary results of Raman spectra from natural diamond samples at elevated temperatures suggest that although the Raman signal associated with the principal first-order phonon mode is significantly broadened, the measured broadening is sub-

6

stantially less than that predicted on the basis of an extrapolation of the data of Krishnan [20]. In addition, we have shown that when the scattering efficiency of the Stokes component decreases as a result of increasing temperature, or when the component suffers from fluorescence interference, the anti-Stokes signal can be be an alternative diagnostic.

The location of the line center in either the Stokes or anti-Stokes component can be an accurate temperature calibrant. We have found that when the diamond substrate is independently heated by a fixed source of power (i.e., foil heater), altering the gas phase composition can have a pronounced effect on the heat transfer from the substrate to the gas stream, thereby substantially changing the substrate temperature. Process control will require a correction to the heater supply so as to compensate for this effect.

Finally, we have shown that interfering plasma emission can be overcome by employing gated photon counting strategies in conjunction with modulated cw or pulsed excitation. Although this results in an increase in the Raman scan durations, satisfactory Raman spectra from natural diamond samples exposed to intense diffuse arc discharges can be obtained well within 10 minutes. Dramatic improvements can be made with increased pulsed laser energies. Future experiments will focus on studying in-situ, the polarization anisotropy of the Raman scattered light from epitaxially grown diamond on diamond and cubic boron-nitride substrates.

ACKNOWLEDGEMENTS

REFERENCES

1. M. Yoshikawa, G. Katagiri, H. Ishida, A. Ishitani, M. Ono and K. Matsumura, Appl. Phys. Lett. 55, 2608 (1989)
2. R.J. Nemanich, J.T. Glass, G. Lucovsky, and R.E. Schroder, J. Vac. Sci. Tech. A6, 1783 (1988).
3. R.E. Shroder, R.J. Nemanich, and J.T. Glass, presented at the SPIE-Optics Conference, San Diego, CA August, 1988.
4. R.G. Buckley, T.D. Moustakas, Ling Ye, and J. Varon, J. Appl. Phys. 66, 3595 (1989).
5. C. Ramaswamy, Nature 125, 704 (1930).
6. R. Robertson and J.J. Fox, Nature 125, 704 (1930).
7. S.A. Solin and A.K. Ramdas, Phys. Rev. B 1, 1687 (1970).
8. R.J. Nemanich and S.A. Solin, Phys. Rev. B 20, 392 (1979).
9. D.S. Knight and W.B. White, J. Mater. Res. 4, 385 (1989).
10. F. Adar, Microbeam Analysis, 67 (1981).
11. R. Loudon, Advanc. Phys. 13, 423 (1964).
12. S.J. Harris, Appl. Phys. Lett. 56, 2298 (1990)
13. D. Huang, M. Frenklach, and M. Maroncelli, J. Phys. Chem. 92, 133 (1988).
14. J.C. Angus and C.C. Hayman, Science 241, 913 (1988)
15. K.E. Spear, J. Am. Ceram. Soc. 72, 171 (1989).
16. B.V. Pritsyn, L.L. Bovilov and B.V. Derjagvin, J. Cryst. Growth 52, 219 (1981)
17. A.A. Maradudin and A.E. Fein, Phys. Rev. 128, 2589 (1962).
18. K.S. Viswanathan, Canad. J. Phys. 41, 423 (1963).
19. P.G.N. Nayar, Proc. Indian Acad. Sci. Sect. A, 13, 284 (1941).
20. R.S. Krishnan, Proc. Indian Acan Sci. Sect. A, 24, 45 (1946).
21. S. Matsumoto, H. Hino and T. Kobayashi, Appl. Phys. Lett. 51, 737 (1987).
22. M.A. Cappelli, T.G. Owano and C.H. Kruger, J. Mater. Res., Nov. (1990), in press
23. M. Yoshikawa, H. Ishida, A. Ishitani, T. Murakami, S. Koizumi and T. Inuzuka, Appl. Phys. Lett. 57, 428 (1990).

7

Dr. W. Adler
General Research Inc.
P. O. Box 6770
Santa Barbara, CA 93160

R. A. Heinecke
Standard Telecommunication
Laboratories, Ltd.
London Road
Harlow, Essex CM17 9MA
England

Mr. D. Roy
Coors Porcelain Co.
Golden, CC 80401

Dr. Mufit Akinc
Mat'ls Science & Eng. Dept.
Iowa State University
110 Engineering Annex
Ames, IA 50011

Dr. Lisa C. Klein
Center for Ceramics Research
College of Engineering
Rutgers University
P. O. Box 909
Piscataway, NJ 08854

Dr. D. Roy
Mat'ls Science Lab
Pennsylvania State Univ.
University Park, PA 16802

Dr. H. E. Bennett
Code 38101
Naval Weapons Center
China Lake, CA 93555

Dr. P. Klocek
Texas Instruments
P. O. Box 660246
Dallas, TX 75266

Dr. J. Savage
Royal Signals & Radar Establishment
St. Andrews Road
Great Malvern, WORCS, WR14 3PS
ENGLAND

Dr. S. Block
Group Leader
Structural Chemistry
National Bureau of Standards
Gaithersburg, MD 20899

Dr. R. Messier
Pennsylvania State University
Materials Research Lab
University Park, PA 16802

Dr. A. Stacy
Chemistry Departament
Univ. of Calif. Berkeley
Berkeley, CA 94720

Dr. J. Burdett
Chemistry Department
University of Chicago
Chicago, IL 60637

Dr. G. Messing
Materials Research Department
Pennsylvania State University
University Park, PA 16802
(1 copy for distribution)

Dr. I. G. Talmy, Code R31
Naval Surface Weapons Center
White Oak Laboratory
Silver Spring, MD 20903

Dr. Mark A. Cappelli
Mechanical Engineering Dept.
Stanford University
Stanford, CA 94305

Dr. S. Musikant
General Electric Company
P. O. Box 8555
Philadelphia, PA 19101

Dr. R. Tustison
Raytheon Co., Research Div.
131 Spring Street
Lexington, MA 02173

Dr. J. A. Cox
Honeywell Systems & Research
Dept. MN 65-2600
3660 Technology Drive
Minneapolis, MN 55418

Dr. Dale Perry
U.S. Army Missile Command
Redstone Arsenal
Huntsville, AL 35807

Dr. W. White
Materials Research Lab
Pennsylvania State Univ.
University Park, PA 16802

Dr. B. Dunn
Materials Science & Eng. Dept.
Univ. of California, Los Angeles
Los Angeles, CA 90024

Dr. W. Pittman
AMSI-RD-AS-PM
Redstone Arsenal
Huntsville, AL 35898

Dr. A. Wold
Chemistry Department
Brown University
Providence, RI 02912

Naval Surface Weapons Ctr
10901 New Hampshire Ave
White Oak Laboratory

Dr. A. Harker
Rockwell International
P. O. Box 1085
1049 Camino Dos Rios
Thousand Oaks, CA 91360

Dr. R. Raj
Materials Science&Eng. Dept.
Cornell University
Ithaca, NY 14853

Capt. Ken L. Yates
AD/AFATL/AGA
Eglin AFB, FL 32542

Office of Naval Research
800 N. Quincy Street
Arlington, VA 22217
Attn:Code1113(H.Guard)
* * * * * * * *'(D.Nelson)

Dr. D. C. Harris (Code 3854)
Naval Weapons Center
China Lake, CA 93555
(1 copy for distribution)

Dr. W. Rhodes
GTE Laboratories
40 Sylvan Road
Waltham, MA 02134

Defense Documentation Center
Cameron Station
Alexandria, VA 22314
(12)

Dr. R. W. Schwartz
Code 373
Naval Weapons Center
China Lake, CA 93555-6001

Naval Air Systems Cmd
1411 Jeff Davis Hwy.
Arlington, VA 22202
Attn:Code 931A (L.Sloter)

Scientific Advisor
Commandant of the
MarineCorps(CodeAX)
Washington,DC 20380

Office of Naval Technology
800 N. Quincy Street
Arlington, VA 22217
Attn:Code 0712(1) Code 0725 (1)